

Application of the I-Effective Method in Calculating Deflections of Partially Prestressed Members



Dan E. Branson

Professor of Civil Engineering,
University of Iowa, Iowa City. In
1980-81, Alexander von Humboldt
U.S. Senior Scientist, Technical
University (RWTH) Aachen,
Federal Republic of Germany.



Heinrich Trost

Professor of Civil Engineering
and Chairman of the Structural
Concrete Institute, Technical
University (RWTH) Aachen,
Federal Republic of Germany.

For computing curvatures and deflections of partially cracked members, the effective moment of inertia (I_e , I_e) method^{1,2,3} provides a transition value between well-defined limits in the uncracked (I_{ucr} or I_g) and fully cracked (I_{cr}) states.

The method is applicable to short-time deflections of non-prestressed and prestressed members alike, and empirically accounts for the effect of tension stiffening (increased stiffness due to concrete in tension, including between cracks). It is also applicable to individual sections, to simple beams, and between inflection points of continuous beams; so that a practical solution that takes into account the random distribution of cracks for all cases, including non-uniform members, is available. The

method is similar to the approach^{4,5} of determining the partially cracked deflection as an intermediate value between the uncracked (State I) and fully cracked (State II) deflections.

The *I*-effective method has been adopted for the 1971 and 1977 ACI Building Codes,⁶ the 1971 and 1978 PCI Design Handbooks,⁷ the 1973 and 1977 AASHTO Highway Bridge Specifications,⁸ and the 1977 Canadian Building Code.⁹ However, its application to non-prestressed and prestressed members has been somewhat different in the past,³ with the live load I_e for prestressed members determined from the prestress plus dead load deflection point, as shown in Fig. 1, and not from the zero deflection point, as in the non-prestressed case using the dead

Synopsis

Unified I -effective procedures for partially cracked non-prestressed and prestressed member curvatures and deflections are summarized. Deflections computed by numerical integration of curvatures (using I_e in the fourth power equation), and also by direct calculation (using I_e in the third power equation) are illustrated for a

typical single-T beam designed as a partially prestressed member in accordance with the ACI Code.

The numerical integration procedure readily lends itself to computer solution for both determinate and indeterminate structures. Results by the two methods are seen to be in close agreement.

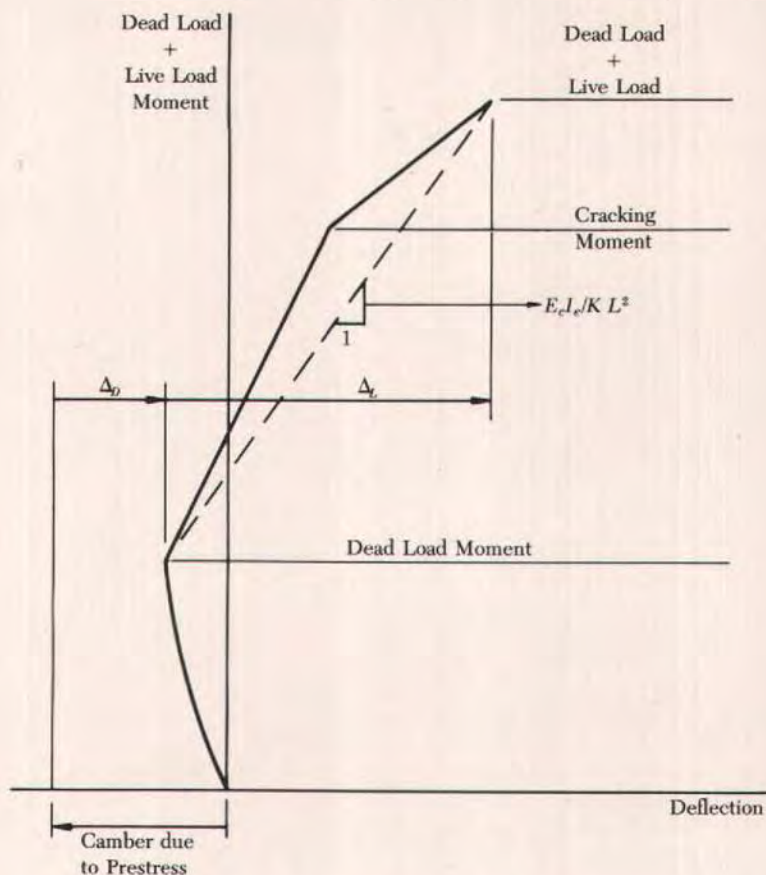


Fig. 1. Moment versus deflection for a partially cracked prestressed member as previously computed by the I_e method.

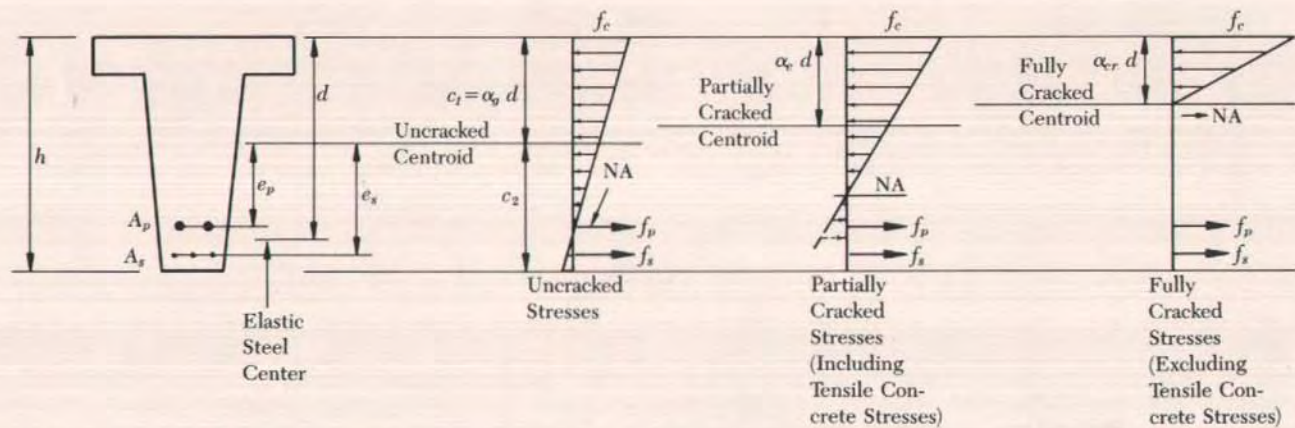
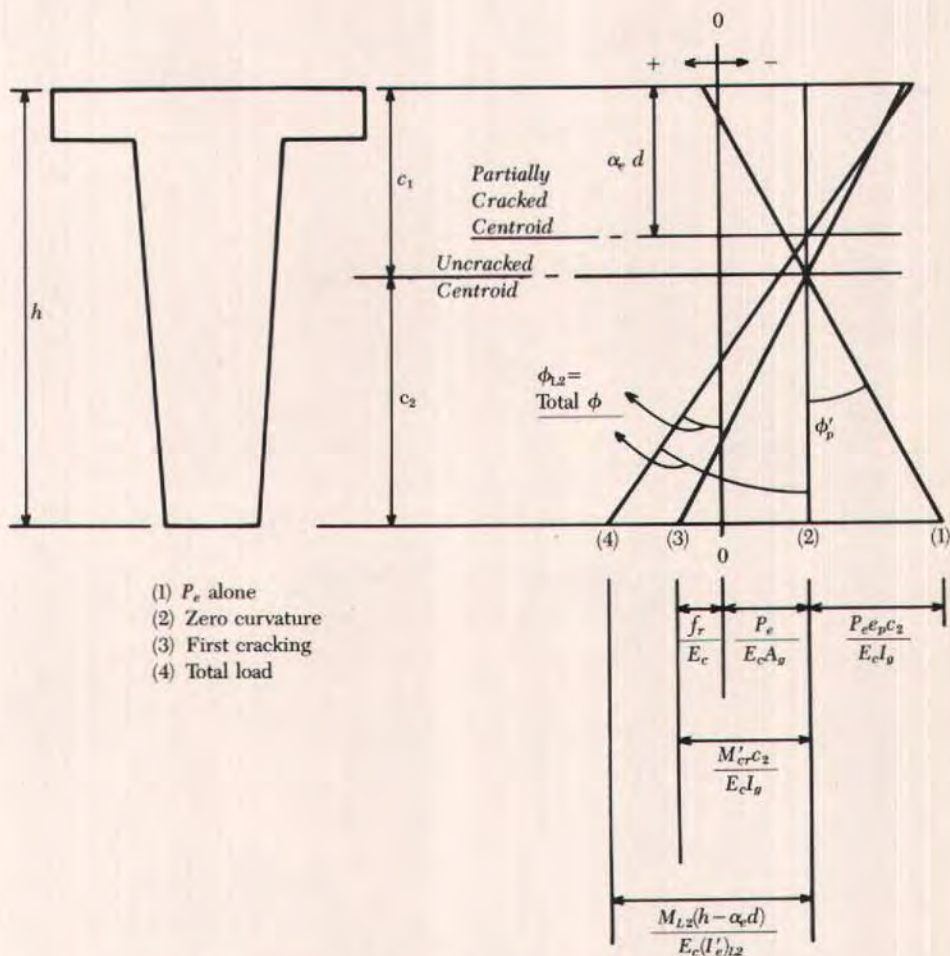


Fig. 2. Basic stress distribution diagrams for uncracked, partially cracked and fully cracked prestressed members, with the location of the centroidal and neutral axes shown.



- (1) P_e alone
- (2) Zero curvature
- (3) First cracking
- (4) Total load

Fig. 3. Strains and curvatures for the general case of a member loaded into the cracking range.

load plus live load I_e . The basic method has been shown to apply to first loading cases and to the envelope of repeated loading cases for at least 313 beams and slabs and 21 different authors.¹¹

In this paper, unified procedures for computing partially cracked non-prestressed and prestressed (with or without non-prestressed tension steel) member curvatures and deflections are

summarized and illustrated by an example of a partially prestressed member designed in accordance with the ACI Code.⁶

The analytical and experimental development of these unified procedures is described in Refs. 10 and 11 in which the procedures were found to apply to load levels well beyond the usual service load range.

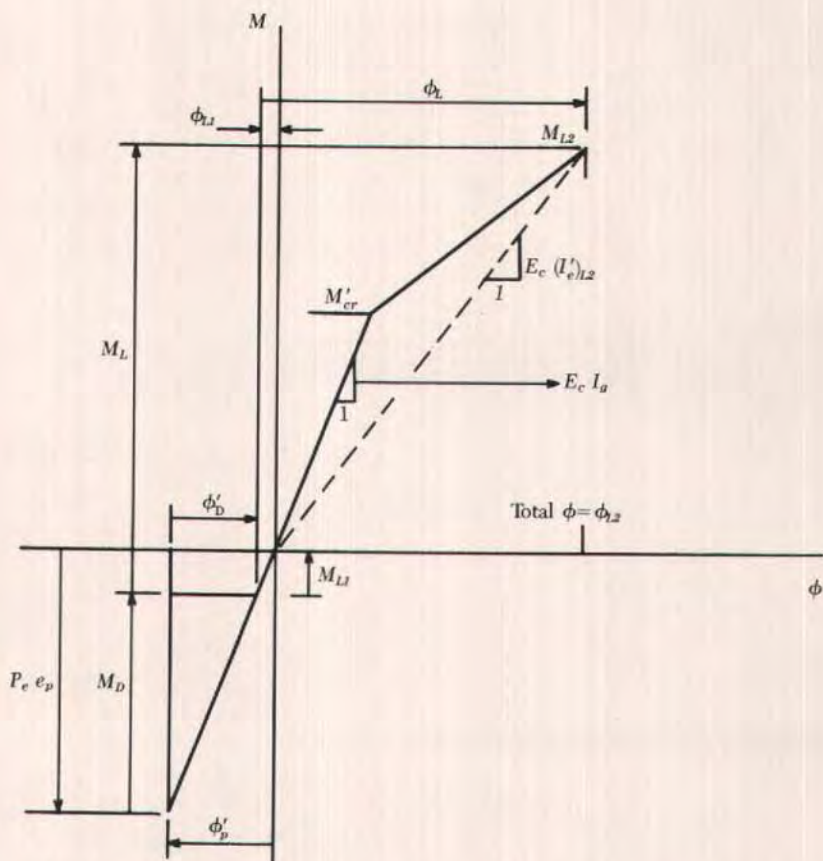


Fig. 4. Idealized moment versus curvature for a prestressed member loaded into the cracking range, in which typical prestress, dead load and live load effects are shown.

UNIFIED PROCEDURES FOR PARTIALLY CRACKED NON-PRESTRESSED AND PRESTRESSED MEMBER CURVATURES AND DEFLECTIONS

This case applies to the condition:

$$(M_D + M_L - P_e e_p > M'_{cr})$$

The basic stress distribution diagrams for uncracked, partially cracked and fully cracked members, with the location of the centroidal and neutral axes,

are shown in Fig. 2 for a prestressed member. The partially cracked state includes empirically the effect of tensile concrete, including in small moment regions, from the top of each crack to the neutral axis, and also between cracks, referred to as tension stiffening.

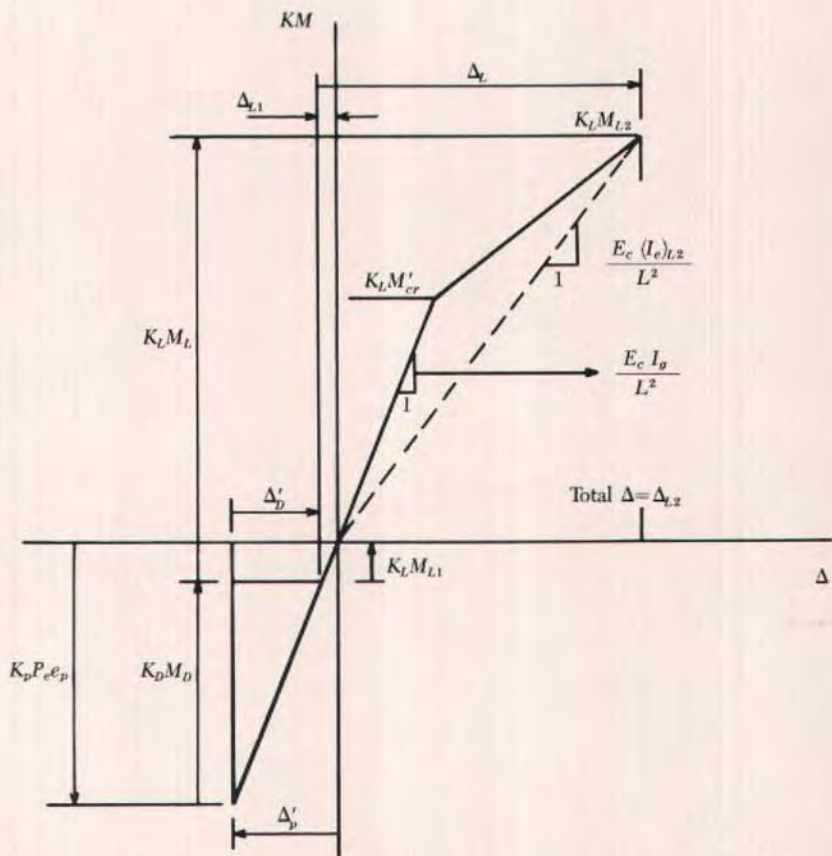


Fig. 5. Idealized deflection coefficient, moment product versus deflection for a prestressed member loaded into the cracking range, in which typical prestress, dead load and live load effects are shown.

In this procedure, which includes the effect of the normal force P_e in the calculation of the cracking moment, the fully cracked section is still taken in the limit to be the lower bound state, as shown in Fig. 2; that is, I_{cr} is the lower limit of I'_e and I_e for both non-prestressed and prestressed cases. The effect of any non-prestressed tension steel in prestressed members is included in the calculation of I_{cr} . As de-

scribed in Refs. 10 and 11, the solution for non-prestressed members follows automatically in the unified procedure by simply setting the prestress force equal to zero.

For the general case of a member loaded into the cracking range, the strains and curvatures are shown in Fig. 3, and the idealized moment-curvature and moment-deflection curves are shown in Figs. 4 and 5.

Curvature at a Particular Section

From distribution line (1) in Fig. 3, the curvature due to prestress is given by Eq. (1) and shown in Fig. 4:

$$\phi_p' = P_e e_p / E_c I_g \quad (1)$$

In the case of statically indeterminate prestressed structures, $\phi_p' = M_{bv}' / E_c I_g$, where $M_{bv}' = M_{bv}^o + M_{bv}'$ includes both determinate and indeterminate moments due to prestress. Although the remainder of the development herein pertains to statically determinate cases, the procedures are equally applicable to indeterminate cases. The initial curvature due to the prestress force at transfer, P_i , is given by Eq. (2):

$$\phi_p = \phi_p' (E_c / E_{ci}) (P_i / P_e) \quad (2)$$

The dead load curvature is given by Eq. (3) at the time under investigation (shown in Fig. 4), and by Eq. (4) initially:

$$\phi_D' = M_D / E_c I_g \quad (3)$$

$$\phi_D = \phi_D' (E_c / E_{ci}) \quad (4)$$

Distribution line (2) in Fig. 3 corresponds to the condition of zero curvature, as shown in Fig. 4 and defined by Eqs. (5), (6) and (7).

From $M_D + M_{L1} - P_e e_p = 0$:

$$M_{L1} = P_e e_p - M_D \quad (5)$$

and

$$\phi_{L1} = \phi_p' - \phi_D' \quad (6)$$

In this uncracked region:

$$\phi_{L1} = M_{L1} / E_c I_g \quad (7)$$

where M_{L1} is the part of the live load moment necessary to produce the zero curvature.

From distribution line (3) in Fig. 3, corresponding to first cracking, Eq. (8) is obtained. The cracking moment, M_{cr}' ,

is also shown in Fig. 4 and refers to the moment above zero, or the net positive moment, required to crack the section:

$$\frac{M_{cr}' c_2}{E_c I_g} = \frac{f_r}{E_c} + \frac{P_e}{E_c A_g} \quad (8)$$

Solving:

$$M_{cr}' = \frac{f_r I_g}{c_2} + \frac{P_e I_g}{A_g c_2} \quad (9)$$

The determination of the cracking moment is further discussed in Refs. 3, 11, 12 and 13.

From distribution line (4) in Fig. 3, corresponding to the total load, and from Fig. 4, Eqs. (10) and (11) are obtained:

$$M_{L2} = M_L - M_{L1} \quad (10)$$

$$\phi_{L2} = M_{L2} / E_c (I_e')_{L2} \quad (11)$$

where M_{L2} is the total live load moment at the section, M_L , minus M_{L1} in Eq. (5). The effective moment of inertia at a particular section, I_e' , in Eq. (11) is shown in Fig. 4 and computed by Eq. (12). By definition:^{1,2,3,10,11}

$$(I_e')_{L2} = \left(\frac{M_{cr}'}{M_{L2}} \right)^4 I_g + \left[1 - \left(\frac{M_{cr}'}{M_{L2}} \right)^4 \right] I_{cr} \leq I_g \quad (12)$$

where M_{cr}' is computed in Eq. (9) and M_{L2} in Eq. (10).

From Fig. 4 and Eq. (6):

$$\text{Total } \phi = -\phi_p' + \phi_D' + \phi_{L1} + \phi_{L2} = \phi_{L2} \quad (13)$$

and

$$\phi_L = \phi_{L1} + \phi_{L2} \quad (14)$$

Deflection of a Beam

Analogous to the above developments for curvatures, the corresponding deflections are shown in Fig. 5 and computed

in the following equations. This figure is presented in terms of KM versus Δ in order that the single line with Slope = $E_c I_g / L^2$ in Fig. 5 can be applied to the deflection under different load distributions (different K 's), such as due to prestress, dead load and live load in a typical problem.

Analogous to Eqs. (1) to (4) due to prestress and dead load:

$$\Delta'_p = K_p P_e e_p L^2 / E_c I_g \quad (15)$$

$$\Delta_p = \Delta'_p (E_c / E_{c1}) (P_i / P_e) \quad (16)$$

$$\Delta'_D = K_D M_D L^2 / E_c I_g \quad (17)$$

$$\Delta_D = \Delta'_D (E_c / E_{c1}) \quad (18)$$

Analogous to Eq. (5), and as shown in Fig. 5, for zero deflection:

$$K_L M_{L1} = K_p P_e e_p - K_D M_D \quad (19)$$

and

$$M_{L1} = (K_p / K_L) P_e e_p - (K_D / K_L) M_D \quad (20)$$

Also from Fig. 5:

$$\Delta_{L1} = \Delta'_p - \Delta'_D \quad (21)$$

In this uncracked region:

$$\Delta_{L1} = K_L M_{L1} L^2 / E_c I_g \quad (22)$$

Eqs. (21) and (22) correspond to Eqs. (6) and (7) for curvatures, respectively.

Analogous to Eqs. (10) and (11), and as shown in Fig. 5, for the total load:

$$K_L M_L = K_L M_{L1} + K_L M_{L2} \quad (23a)$$

$$M_{L2} = M_L - M_{L1} \quad (23b)$$

and

$$\Delta_{L2} = K_L M_{L2} L^2 / E_c (I_e)_{L2} \quad (24)$$

The average effective moment of inertia for a beam, I_e , in Eq. (24) is shown in Fig. 5 and computed by Eq. (25). By definition:^{1,2,3,10,11}

$$(I_e)_{L2} = \left(\frac{M'_{cr}}{M_{L2}} \right)^3 I_g + \left[1 - \left(\frac{M'_{cr}}{M_{L2}} \right)^3 \right] I_{cr} \leq I_g \quad (25)$$

where M'_{cr} is computed in Eq. (9) and M_{L2} in Eq. (10).

From Fig. 5 and Eq. (21):

$$\text{Total } \Delta = -\Delta'_p + \Delta'_D + \Delta_{L1} + \Delta_{L2} = \Delta_{L2} \quad (26)$$

and

$$\Delta_L = \Delta_{L1} + \Delta_{L2} \quad (27)$$

In the above equations for computing deflections, the bending moments are usually the maximum moments for simple spans and the maximum moments between inflection points for continuous spans, with the deflection coefficients, K , defined accordingly.

DESIGN EXAMPLE — SIMPLE SPAN PARTIALLY PRESTRESSED SINGLE-T BEAM

Design Details and Stress Analysis

The design conditions, properties, loads and moments are shown in Table 1, and the design details are depicted in Fig. 6. The design is shown to be satisfactory based on the ACI Code allowable stresses for partially prestressed members.

$$P_i = f_{pi} A_p = (1302 \text{ MN/m}^2) (0.0016 \text{ m}^2) \\ = 2.083 \text{ MN (468 kips)}$$

$$P_e = f_{pe} A_p = (1042) (0.0016) \\ = 1.667 \text{ MN (375 kips)}$$

Concrete stresses at transfer:

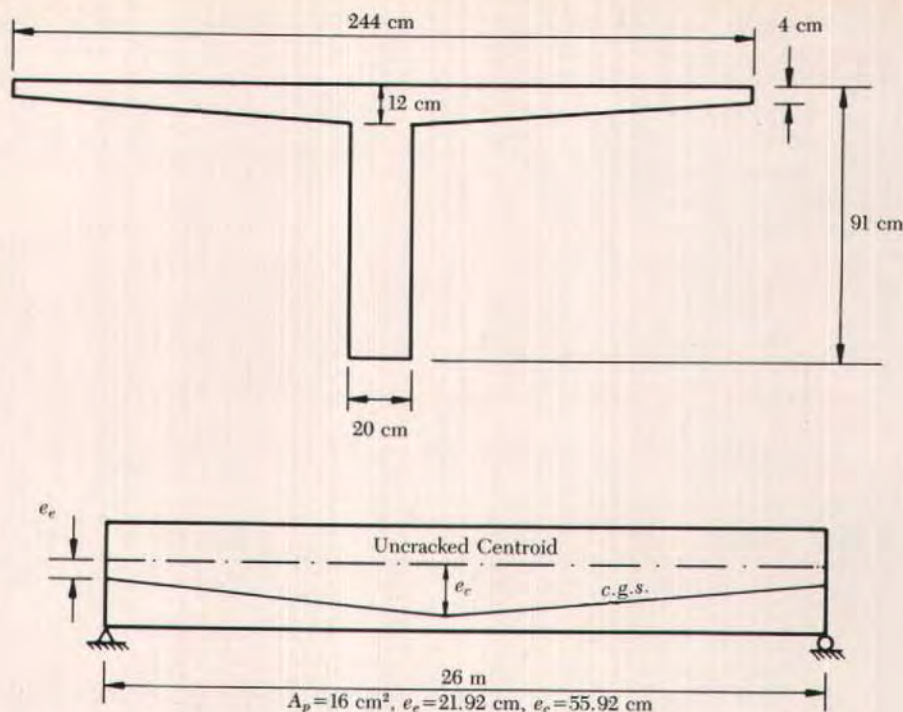


Fig. 6. Single-T partially prestressed beam in the Example.

$$\begin{aligned} \text{End } f_1 &= -\frac{P_1}{A_g} + \frac{P_1 e_e}{S_1} \\ &= -\frac{2.083}{0.3612} + \frac{(2.083)(0.2192)}{0.1117} \\ &= -5.77 + 4.09 = -1.68 \text{ MN/m}^2 \\ &= -1.68 \text{ MPa (244 psi)} \end{aligned}$$

$$\begin{aligned} \text{End } f_2 &= -\frac{P_1}{A_g} - \frac{P_1 e_e}{S_2} \\ &= -5.77 - \frac{(2.083)(0.2192)}{0.04248} \\ &= -5.77 - 10.75 \\ &= -16.52 \text{ MPa (2396 psi)} \end{aligned}$$

$$\begin{aligned} \text{Midspan } f_1 &= -\frac{P_1}{A_g} + \frac{P_1 e_c}{S_1} - \frac{M_D}{S_1} \\ &= -5.77 + \frac{(2.083)(0.5592)}{0.1117} - \frac{0.722}{0.1117} \\ &= -5.77 + 10.43 - 6.46 \\ &= -1.80 \text{ MPa (261 psi)} \end{aligned}$$

$$\begin{aligned} \text{Midspan } f_2 &= -\frac{P_1}{A_g} - \frac{P_1 e_c}{S_2} + \frac{M_D}{S_2} \\ &= -5.77 - \frac{(2.083)(0.5592)}{0.04248} + \frac{0.722}{0.04248} \\ &= -5.77 - 27.42 + 17.00 \\ &= -16.19 \text{ MPa (2348 psi)} \end{aligned}$$

The above stresses are now compared to the following ACI Code allowable stresses:

$$\begin{aligned} \text{Compression at transfer} &= 0.60 f'_{ct} \\ &= (0.60)(28) \\ &= 16.80 \text{ MPa} \\ &= (2437 \text{ psi}) \end{aligned}$$

$$\begin{aligned} \text{Tension at transfer} &= 3 \sqrt{f'_{ct}}, \text{ psi} \\ &= 0.2491 \sqrt{f'_{ct}}, \text{ MPa} \\ &= 0.2491 \sqrt{28} \\ &= 1.32 \text{ MPa (191 psi)} \end{aligned}$$

Table 1. Design conditions, properties, loads and moments for design example.

Material Properties (ACI)
Steam cured normal weight concrete—Unit weight = 2320 kg/m ³ x 1.04 to include extra weight of steel = 2410 kg/m ³ (150 pcf)
$f'_{ci} = 28$ MPa (4060 psi), $f'_c = 34$ MPa (5080 psi), $f_{pu} = 1860$ MPa (270 K)
$f_{pi} = 0.70 f_{pu} = 1302$ MPa (189 ksi), Assume $f_{pe} = 0.80 f_{pi} = 1042$ MPa (151 ksi)
$f_r = 7.5 \sqrt{f'_c}$, psi = $0.6228 \sqrt{f'_c}$, MPa = $0.6228 \sqrt{35} = 3.68$ MPa (534 psi)
$E_{ci} = 57,600 \sqrt{f'_{ci}}$, psi = $4783 \sqrt{f'_{ci}}$, MPa = $4783 \sqrt{28} = 25,310$ MPa (3.67×10^6 psi)
$E_c = 4783 \sqrt{f'_c} = 4783 \sqrt{35} = 28,300$ MPa (4.10×10^6 psi)
$E_p = 186,000$ MPa (27.0×10^6 psi for strand), $n = E_p/E_c = 186,000/28,300 = 6.57$
Section Properties
$c_2 = 65.92$ cm, $c_1 = 91 - c_2 = 25.08$ cm
$e_e = 21.92$ cm, $d = 91 - \text{say } 10 = 81.00$, $e_c = d - c_1 = 55.92$ cm
$A_g = 3612$ cm ² , $I_g = 2,800,200$ cm ⁴
$S_1 = I_g/c_1 = 111,700$ cm ³ , $S_2 = I_g/c_2 = 42,480$ cm ³
Considering only the rectangular flange in compression (neglecting the taper),
$(244) (4) (\alpha_{cr} d - 2) = (6.57) (16) (81.00 - \alpha_{cr} d)$
Solving, $\alpha_{cr} d = 9.68$ cm
$I_{cr} = (244) (4)^3/12 + (244) (4) (9.68 - 2)^2 + (6.57) (16) (81.00 - 9.68)^2 = 593,600$ cm ⁴
(USE) (versus correct value of 599,900 cm ⁴)
Loads and Moments
$w_D = (0.3612 \text{ m}^2) (2410 \text{ kg/m}^3) (0.008907 \text{ kN/kg}) = 8.54 \text{ kN/m}$ (585 lb/ft)
Assume $w_L = 7.5 \text{ kN/m}$ (3.07 kN/m ² , 514 lb/ft, 64.1 psf)
$M_D = w_D L^2/8 = (8.54) (26)^2/8 = 722 \text{ kN-m}$ (532 ft-k)
$M_L = w_L L^2/8 = (7.5) (26)^2/8 = 634 \text{ kN-m}$ (468 ft-k)
Total Gravity Load Moment = $M_{D+L} = 1356 \text{ kN-m}$ (1000 ft-k)

Hence, the computed stresses at transfer are satisfactory.

Concrete stresses after losses with live load:

$$\begin{aligned} \text{Midspan } f_1 &= -\frac{P_e}{A_g} + \frac{P_e e_c}{S_1} - \frac{M_{D+L}}{S_1} \\ &= -\frac{1.667}{0.3612} + \frac{(1.667)(0.5592)}{0.1117} - \frac{1.356}{0.1117} \\ &= -4.62 + 8.35 - 12.14 \\ &= -8.41 \text{ MPa (1220 psi)} \end{aligned}$$

$$\begin{aligned} \text{Midspan } f_2 &= -\frac{P_e}{A_g} - \frac{P_e e_c}{S_2} + \frac{M_{D+L}}{S_2} \\ &= -4.62 - \frac{(1.667)(0.5592)}{0.04248} + \frac{1.356}{0.04248} \\ &= -4.62 - 21.94 + 31.92 \\ &= +5.36 \text{ MPa (777 psi)} \end{aligned}$$

The computed stresses are again compared with the following ACI Code allowable stresses:

$$\begin{aligned} \text{Compression after losses:} \\ &= 0.45 f'_c \\ &= (0.45) (35) \\ &= 15.75 \text{ MPa (2284 psi)} \end{aligned}$$

$$\begin{aligned} \text{Tension after losses:} \\ > f_r = 3.68 \text{ MPa (534 psi) (Table 1)} \\ < 12 \sqrt{f'_c}, \text{ psi} \\ < 0.9965 \sqrt{f'_c}, \text{ MPa} \\ &= 0.9965 \sqrt{35} = 5.90 \text{ MPa (856 psi)} \end{aligned}$$

According to the ACI Code, the computed stresses after losses are satisfactory, except that the live load deflection must be computed by a bilinear partially prestressed method (partially cracked section).

Table 2. Numerical solution for design example
(Hand calculations by Newmark numerical procedure¹⁴).

Description									Multiplier, Units	
	$L/2 = 13 \text{ m}$ 3.25 m 3.25 m 3.25 m 3.25 m									
Section No.	0	1	2	3	4	5	6	7	—	
e_p	21.92	30.42	38.92	47.42	55.92	64.42	72.92	81.42	cm	
$d = e_p + c_1 = e_p + 25.08 =$	47.00	55.50	64.00	72.50	81.00	89.50	98.00	106.50	cm	
$\alpha_{cr} d$	6.38	7.20	8.03	8.85	9.68	10.50	11.32	12.15	cm	
I_{cr}	193,500	272,900	366,100	473,000	593,600	728,000	877,000	1,040,000	cm ⁴	
$\phi'_p = P_e e_p / E_c I_p$ [Eq. (1)]	0.	4611	0.	6399	0.	8187	0.	9975	1.763	10^{-3} 1/m
$\overline{\phi'_p}$ (see Footnote 1)	—		2.080	2.661	3.242	3.823	4.404	4.985	629 x 10^{-3}	Dimensionless
Slope (starting with half of center value)	—	9.798	7.718	5.057	1.815					Dimensionless
Deflection, Δ'_p	0	9.798	17.516	22.573	24.388	23.888	21.388	17.888	3250 x 10^{-3}	mm
Deflection, Δ'_p	0	31.8	56.9	73.4	79.3	74.3	58.3	32.3		mm
M_D	0	315.9	541.5	676.9	722.0	676.9	541.5	315.9	0	kN-m
$\phi'_D = M_D / E_c I_p$ [Eq. (3)]	0	0.3986	0.6833	0.8542	0.9111	0.8542	0.6833	0.3986	0.9111	10^{-3} 1/m
$\overline{\phi'_D}$ (see Footnote 2)	—	1.265	2.190	2.745	2.930	2.745	2.190	1.265	930 x 10^{-3}	Dimensionless
Slope (starting with half of center value)	—	7.665	6.400	4.210	1.465					Dimensionless
Deflection, Δ'_D	0	7.665	14.065	18.275	19.740	17.275	12.065	7.665	740	3250×10^{-3}
Deflection, Δ'_D	0	24.9	45.7	59.4	64.2	59.4	45.7	24.9		mm
$M_{L1} = P_e e_p - M_D$ [Eq. (5)]	365.4	191.2	107.3	113.6	210.6	210.6	113.6	107.3	191.2	kN-m
$\phi_{L1} = M_{L1} / E_c I_p$ [Eq. (7)]	0.4611	0.2413	0.1354	0.1433	0.2653	0.2653	0.1433	0.2413	0.2413	10^{-3} 1/m
M_L	0	277.4	475.5	594.4	634.0	594.4	475.5	277.4	0	kN-m
$M_{L2} = M_L - M_{L1}$ [Eq. (10)]	-365.4	86.2	368.2	480.8	423.8	368.2	247.8	86.2	86.2	kN-m
M'_{cr} / M_{L2} (see Footnote 3)	—	> 1	0.9571	0.7329	0.8315	0.8315	0.7329	0.9571	0.8315	Dimensionless
$(M'_{cr} / M_{L2})^*$	—	> 1	0.839	0.289	0.478	0.478	0.289	0.839	0.478	Dimensionless
$(I'_c)_{L2}$ (Eq. 12)	2.800	2.800	2.445	1.231	1.648	1.648	1.231	2.445	2.800	10^6 cm^4
$\phi_{L2} = M_{L2} / E_c (I'_c)_{L2}$ [Eq. (11)]	-0.4611	0.1088	0.5321	1.3801	0.9087	0.9087	1.3801	0.1088	0.1088	10^{-3} 1/m
$\phi_L = \phi_{L1} + \phi_{L2}$ [Eq. (14)]	0.0000	0.3501	0.6675	1.5234	1.1740	1.1740	1.5234	0.3501	0.3501	10^{-3} 1/m
$\overline{\phi_L}$ (see Footnote 2)	—	1.129	2.315	4.625	4.005	4.005	2.315	1.129	0.005 x 10^{-3}	Dimensionless
Slope (starting with half of center value)	—	10.072	8.943	6.628	2.003					Dimensionless
Deflection, Δ_L	0	10.072	19.015	25.643	27.646	25.643	19.015	10.072	3250 x 10^{-3}	mm
Deflection, Δ_L	0	32.7	61.8	83.3	89.9	83.3	61.8	32.7		mm

See notes on opposite page.

Uncracked Beam Deflection Computed by Numerical Integration of Elastic Curvatures (M/EI_g). Cracked beam deflection computed by numerical integration of curvatures using I'_g (with 4th power equation) Fig. 4

The following sample calculations pertain to Section 4 in Table 2:

$$\alpha_{cr} d = 9.68 \text{ cm (3.81 in.)}$$

(Calculation shown in Table 1)

$$I_{cr} = 593,600 \text{ cm}^4 \text{ (14,260 in.}^4\text{)}$$

(Calculation shown in Table 1)

$$\begin{aligned} \phi_p' &= P_e e_p / E_c I_g && \text{Eq. (1)} \\ &= \frac{(1.667)(0.5592)}{(28,300)(0.028002)} \\ &= 1.1763 \times 10^{-3} \text{ 1/m} \\ &\quad (0.359 \times 10^{-3} \text{ 1/ft}) \end{aligned}$$

As shown in Footnote 1 of Table 2:

$$\begin{aligned} \bar{\phi}_p' &= \frac{3.25}{6} \\ &\quad (0.9975 + 4 \times 1.1763 + 0.9975) 10^{-3} \\ &= 3.629 \times 10^{-3} \text{ (dimensionless)} \end{aligned}$$

From Table 2:

Midspan $\Delta_p' = 79.3 \text{ mm (3.13 in.)}$
which is exactly the same as the result by the direct calculation method (next section). The reason for this is shown in Footnote 1 of Table 2.

$$\begin{aligned} M_D &= 722 \text{ kN-m (532 ft-k)} \\ &\quad \text{(calculation shown in Table 1)} \\ \phi_D' &= M_D / E_c I_g && \text{Eq. (3)} \\ &= \frac{0.722}{(28,300)(0.028002)} \\ &= 0.9111 \times 10^{-3} \text{ 1/m (0.278} \times 10^{-3} \text{ 1/ft)} \end{aligned}$$

As shown in Footnote 2 of Table 2:

$$\begin{aligned} \bar{\phi}_D' &= \frac{3.25}{12} \\ &\quad (0.8542 + 10 \times 0.9111 + 0.8542) 10^{-3} \\ &= 2.930 \times 10^{-3} \text{ (dimensionless)} \end{aligned}$$

From Table 2:

Midspan $\Delta_D' = 64.2 \text{ mm (2.53 in.)}$
which is exactly the same as the result by the direct calculation method (next section). The reason for this is shown in Footnote 2 of Table 2.

$$\begin{aligned} M_{L1} &= P_e e_p - M_D && \text{Eq. (5)} \\ &= (1667)(0.5592) - 722 \\ &= 210.2 \text{ kN-m (155 ft-k)} \end{aligned}$$

$$\begin{aligned} \phi_{L1} &= M_{L1} / E_c I_g && \text{Eq. (7)} \\ &= \frac{0.2102}{(28,300)(0.028002)} \\ &= 0.2653 \times 10^{-3} \text{ 1/m} \\ &\quad (0.0809 \times 10^{-3} \text{ 1/ft)} \end{aligned}$$

$$\begin{aligned} M'_{cr} &= \frac{f_r I_g}{c_2} + \frac{P_e I_g}{A_g c_2} && \text{Eq. (9)} \\ &= \frac{(3.68)(0.028002)}{0.6592} + \frac{(1.667)(0.028002)}{(0.3612)(0.6592)} \end{aligned}$$

$$\begin{aligned} &= 0.3524 \text{ MN-m} \\ &= 352.4 \text{ kN-m (260 ft-k)} \end{aligned}$$

$$\begin{aligned} M_{L2} &= M_L - M_{L1} && \text{Eq. (10)} \\ &= 634.0 - 210.2 \\ &= 423.8 \text{ kN-m (313 ft-k)} \end{aligned}$$

$$\begin{aligned} (M'_{cr} / M_{L2})^4 &= (352.4 / 423.8)^4 \\ &= 0.8315^4 = 0.478 \end{aligned}$$

$$(I'_e)_{L2} = \left(\frac{M'_{cr}}{M_{L2}} \right)^4 I_g + \text{Eq. (12)}$$

$$\begin{aligned} &\left[1 - \left(\frac{M'_{cr}}{M_{L2}} \right)^4 \right] I_{cr} \leq I_g \\ &= (0.478)(2,800,200) + \\ &\quad (1 - 0.478)(593,600) \\ &= 1,648,400 \text{ cm}^4 \text{ (39,600 in.}^4\text{)} \end{aligned}$$

From Newmark numerical procedure¹⁴ with incremental length = $L/8$:

1. For straight line curvature (M/EI) diagrams (the prestress case in the example), the following is exact:

$$\bar{\phi}_1 = \frac{L/8}{6} (\phi_0 + 4\phi_1 + \phi_2), \quad \bar{\phi}_2 = \frac{L/8}{6} (\phi_1 + 4\phi_2 + \phi_3), \text{ etc.}$$

2. For 2nd degree parabolic curvature (M/EI) diagrams (the dead load case in the example), the following is exact:

$$\bar{\phi}_1 = \frac{L/8}{12} (\phi_0 + 10\phi_1 + \phi_2), \quad \bar{\phi}_2 = \frac{L/8}{12} (\phi_1 + 10\phi_2 + \phi_3), \text{ etc.}$$

For most other cases, the equation is very accurate but not exact (the live load case in the example).

3. Beam is uncracked at the end (at the top under the negative moment). Use I_g at the end section.

$$\phi_{L2} = M_{L2}/E_c (I'_e)_{L2} \quad \text{Eq. (11)}$$

$$= \frac{0.4238}{(28,300) (0.016484)}$$

$$= 0.9087 \times 10^{-3} \text{ 1/m } (0.277 \times 10^{-3} \text{ 1/ft})$$

$$\phi_L = \phi_{L1} + \phi_{L2} \quad \text{Eq. (14)}$$

$$= (0.2653 + 0.9087)10^{-3}$$

$$= 1.1740 \times 10^{-3} \text{ 1/m } (0.358 \times 10^{-3} \text{ 1/ft})$$

As shown in Footnote 2 of Table 2:

$$\bar{\phi}_L = \frac{3.25}{12}$$

$$(1.5234 + 10 \times 1.1740 + 1.5234)10^{-3}$$

$$= 4.005 \times 10^{-3} \text{ (dimensionless)}$$

From Table 2:

Midspan $\Delta_L = 89.9 \text{ mm } (3.54 \text{ in.})$
 versus $89.1 \text{ mm } (3.51 \text{ in.})$ by the direct calculation method in the next section. These results demonstrate the typical close agreement (see Refs. 1 and 3) between the two procedures for uniformly distributed live loading (and similar but to a lesser degree for two or more point loads per span) — using the fourth power equation for I'_e when computing curvatures first and then numerically solving for the deflections, and using the third power equation for I_e when computing deflections directly.

Direct Calculation of Uncracked Beam Deflection. Cracked beam deflection computed directly using the average I_e (with 3rd power equation) Fig. 5

$$\Delta'_p = K_p P_e e_p L^2/E_c I_p, e_p = e_c \quad \text{Eq. (15)}$$

$$= \frac{P_e (e_c - e_e) L^2}{12 E_c I_p} + \frac{P_e e_e L^2}{8 E_c I_p} \quad \text{Ref. (3)}$$

$$= \frac{(1.667) (0.5592 - 0.2192) (26)^2}{(12) (28,300) (0.028002)} +$$

$$\frac{(1.667) (0.2192) (26)^2}{(8) (28,300) (0.028002)}$$

$$= 0.0793 \text{ m} = 79.3 \text{ mm } (3.12 \text{ in.})$$

which is exactly the same as the result by the numerical integration method in the previous section. The reason for this is shown in Footnote 1 of Table 2.

Solving Eq. (15) above, $K_p = 0.0997$.

For uniformly distributed loading:

$$K_D = K_L = 5/48 = 0.1042$$

Checking the conditions of Fig. 5:

$$K_p P_e e_p = (0.0997) (1.667) (0.5592)$$

$$= 0.0929 \text{ MN-m} = 92.9 \text{ kN-m}$$

$$(69 \text{ ft-k})$$

$$> K_D M_D = (5/48) (722)$$

$$= 75.2 \text{ kN-m } (55 \text{ ft-k})$$

$$\Delta_p = \Delta'_p (E_c/E_{ct}) (P_i/P_e) \quad \text{Eq. (16)}$$

$$= (79.3) (28,300/25,310) (2.083/1.667)$$

$$= 111 \text{ mm } (4.37 \text{ in.})$$

$$\Delta'_D = K_D M_D L^2/E_c I_D \quad \text{Eq. (17)}$$

$$= \frac{(5/48) (0.722) (26)^2}{(28,300) (0.028002)}$$

$$= 0.0642 \text{ m} = 64.2 \text{ mm } (2.53 \text{ in.})$$

which is exactly the same as the result by the numerical integration method in the previous section. The reason for this is shown in Footnote 2 of Table 2.

$$\Delta_D = \Delta'_D (E_c/E_{ct}) \quad \text{Eq. (18)}$$

$$= (64.2) (28,300/25,310)$$

$$= 71.8 \text{ mm } (2.83 \text{ in.})$$

$$M_{L1} = (K_p/K_L) P_e e_p - (K_D/K_L) M_D, e_p = e_c$$

$$= \frac{0.0997}{0.1042} (1.667) (0.5592)$$

$$- (1.000) (0.722) \quad \text{Eq. (20)}$$

$$= 0.170 \text{ MN-m} = 170 \text{ kN-m } (125 \text{ ft-k})$$

$$\Delta_{L1} = K_L M_{L1} L^2/E_c I_D \quad \text{Eq. (22)}$$

$$= \frac{(5/48) (0.170) (26)^2}{(28,300) (0.028002)}$$

$$= 0.0151 \text{ m} = 15.1 \text{ mm } (0.59 \text{ in.})$$

$$M_{L2} = M_L - M_{L1} \quad \text{Eq. (23)}$$

$$= 634 - 170$$

$$= 464 \text{ kN-m } (342 \text{ ft-k})$$

$$M'_{cr} = 352.4 \text{ kN-m (260 ft-k)}$$

(calculated in previous section)

$$(M'_{cr}/M_{L2})^3 = (352.4/464)^3$$

$$= 0.7595^3 = 0.438$$

$$(I_e)_{L2} = \left(\frac{M'_{cr}}{M_{L2}} \right)^3 I_g +$$

$$\left[1 - \left(\frac{M'_{cr}}{M_{L2}} \right)^3 \right] I_{cr} \leq I_g \quad \text{Eq. (25)}$$

$$= (0.438)(2,800,200) +$$

$$(1 - 0.438)(593,600)$$

$$= 1,560,100 \text{ cm}^4 (37,480 \text{ in.}^4)$$

$$\Delta_{L2} = K_L M_{L2} L^2 / E_c (I_e)_{L2} \quad \text{Eq. (24)}$$

$$= \frac{(5/48)(0.464)(26)^2}{(28,300)(0.015601)}$$

$$= 0.0740 \text{ m}$$

$$= 74.0 \text{ mm (2.91 in.)}$$

$$\Delta_L = \Delta_{L1} + \Delta_{L2} \quad \text{Eq. (27)}$$

$$= 15.1 + 74.0$$

$$= 89.1 \text{ mm (3.51 in.)}$$

versus 89.9 mm (3.54 in.) by the numerical integration method in the previous section. These results demonstrate the typical close agreement (see Refs. 1 and 3) between the two procedures for uniformly distributed live loading (and similar but to a lesser degree for two or more point loads per span), using the third power equation for I_e when computing deflections directly, and using the fourth power equation for I'_e when computing curvatures first and then numerically solving for the deflections.

The ACI Code allowable deflections for roofs and floors under live load are:

$$\text{Roofs: } L/180 = 26,000/180$$

$$= 144 \text{ mm (5.67 in.)}$$

$$\text{Floors: } L/360 = 72 \text{ mm (2.83 in.)}$$

Based on these limits, the design is satisfactory for roofs but not for floors (Computed $\Delta_L = 89 \text{ mm}$ and 90 mm by the two methods).

CONCLUDING REMARKS

Unified I -effective procedures for partially cracked non-prestressed and prestressed member curvatures and deflections have been summarized. The analytical and experimental development of these procedures is described in Refs. 10 and 11. Both of the procedures empirically account for the effect of tension stiffening.

In this paper the application of the unified procedures is illustrated for a typical single-T beam designed as a partially prestressed member in accordance with the ACI Code, which requires that deflections be computed. The midspan live load deflection is computed as 89.9 mm (3.54 in.) by the numerical integration of curvatures, and 89.1 mm (3.51 in.) by direct calculation.

This demonstrates the typical close (although not always that close) agreement between the two procedures for uniformly distributed loading using the third power equation for I_e when computing deflections directly, and using the fourth power equation for I'_e when computing curvatures first and then numerically solving for the deflections. Such results are consistent with previous results,^{1,3} particularly those of Ref. 1 for non-prestressed members in which the two equations were initially determined empirically.

The design example, analyzed by these methods, is shown to be satisfactory for roofs but not for floors, according to the ACI Code allowable live load deflections.

ACKNOWLEDGMENTS

This paper summarizes part of a research project conducted as a result of a U.S. Senior Scientist Award from the Alexander von Humboldt Foundation of the Federal Republic of Germany. Support was also received from the University of Iowa and the Technical University Aachen. This assistance is greatly appreciated. Thanks are also extended to Dr.-Ing. H. Cordes, Dr.-Ing. J. Frey and Dipl.-Ing. B. Weller for their assistance.

APPENDIX—NOTATION

- A_g = area of gross section, neglecting the steel
 A_p = area of prestressing steel
 c_1, c_2 = distance from uncracked centroid (gross section) to top, bottom surfaces, respectively
 d = effective depth of a beam (distance from compression face to center of steel)
 E_c = modulus of elasticity of concrete at the time the superimposed loading, such as live load, is applied; normally taken to be at age 28 days
 E_{ci} = modulus of elasticity of concrete at the time of initial loading, such as at the time of prestress transfer
 E_p = modulus of elasticity of prestressing steel
 e_c, e_e = eccentricity at midspan, end of a beam, respectively
 e_p = eccentricity of prestressing steel
 f_1, f_2 = flexural stress in concrete at top, bottom surfaces, respectively
 f_{pe} = stress in prestressing steel corresponding to the effective prestress force, P_e , after all losses
 f_{pi} = temporary stress in prestressing steel at transfer (initial prestress)
 f_{pu} = ultimate tensile strength of prestressing steel
 f_r = modulus of rupture of concrete
 f'_c = compressive strength of concrete, normally at age 28 days
 f'_{ci} = compressive strength of concrete at the time of prestress transfer
 I_{cr} = moment of inertia of the fully cracked section
 I_e = effective moment of inertia for deflection
 I'_e = effective moment of inertia for curvature
 $(I'_e)_{L2}, (I_e)_{L2}$ = effective moment of inertia for curvature and deflection, respectively, for the part of the live load moment, M_{L2} , corresponding to a positive curvature (concave upward), deflection (downward)
 I_g = moment of inertia of gross section, neglecting the steel
 I_{ucr} = moment of inertia of uncracked transformed section
 K_D, K_L, K_p = deflection coefficient for dead load moment, live load moment, prestress moment, respectively
 L = span length
 M_{bv} = total bending moment due to prestress
 M_{bv}^o = statically determinate moment due to prestress = $P_e e_p$
 M_{bv}' = statically indeterminate moment due to prestress
 M_{cr}' = cracking moment (moment above zero, or the net positive moment, necessary to crack a beam), as defined by Eq. (9)
 M_D, M_L = dead load moment, live load moment, respectively
 M_{L1} = part of live load moment corresponding to zero curvature, deflection
 M_{L2} = part of live load moment corresponding to positive curvature (concave upward), deflection (downward)
 n = modular ratio
 P_e = effective prestress force (after losses)
 P_i = initial prestress force, or prestress force at transfer
 S_1, S_2 = section moduli of top, bottom surfaces, respectively
 w_D, w_L = uniformly distributed dead load, live load, respectively
 α = ratio of distance from centroid to top surface to d
 $\alpha_{cr} d$ = location of fully cracked centroid
 $\alpha_e d$ = location of partially cracked centroid
 $\alpha_g d$ = location of uncracked (gross section) centroid
 Δ = deflection
 ϕ = curvature
 Δ_D, ϕ_D = deflection, curvature due to dead load
 Δ'_D, ϕ'_D = fictitious deflection, curvature

due to dead load using E_c (rather than E_{ci}) in the calculation

Δ_L, ϕ_L = deflection, curvature due to live load

Δ_{L1}, ϕ_{L1} = part of the live load deflection, curvature which, together with the prestress camber, produces zero deflection, curvature

Δ_{L2}, ϕ_{L2} = part of the live load deflection, curvature corresponding to posit-

ive values (downward deflection, concave upward curvature); also the net or total deflection, curvature

Δ_p, ϕ_p = deflection, curvature due to prestress

Δ'_p, ϕ'_p = fictitious deflection, curvature due to prestress using E_c (rather than E_{ci}) in the calculation

$\bar{\phi}$ = equivalent concentrated angle change in Newmark procedure

REFERENCES

1. Branson, D. E., "Instantaneous and Time-Dependent Deflections of Simple and Continuous Reinforced Concrete Beams," HPR Publication No. 7, Part 1, Alabama Highway Department, U.S. Bureau of Public Roads, August 1963, pp. 1-78.
2. Shaikh, A. F., and Branson, D. E., "Nontensioned Steel in Prestressed Concrete Beams," PCI JOURNAL, V. 15, No. 1, February 1970, pp. 14-36.
3. Branson, D. E., *Deformation of Concrete Structures*, McGraw-Hill International Book Co., Advanced Book Program, New York, St. Louis, San Francisco, Auckland, Bogota, Dusseldorf, Johannesburg, Madrid, London, Mexico, Montreal, New Delhi, Panama, Paris, Sao Paulo, Singapore, Sydney, Tokyo, Toronto, 1977, pp. 1-546.
4. Trost, H., and Mainz, B., "Zweckmässige Ermittlung der Durchbiegung von Stahlbetonträgern" (Deflections of Reinforced Concrete Members), *Beton und Stahlbetonbau*, V. 64, June 1969, pp. 142-146.
5. Trost, H., "The Calculation of Deflections of Reinforced Concrete Beams," *Proceedings, Adrian Pauw Symposium on Designing for Creep and Shrinkage in Concrete Structures*, American Concrete Institute, Houston, Texas, November 1978, pp. 1-9.
6. ACI Committee 318, "Building Code Requirements for Reinforced Concrete (ACI 318-77)," American Concrete Institute, Detroit, Michigan, 1977, pp. 1-102.
7. *PCI Design Handbook - Precast, Prestressed Concrete*, 2nd Edition, Prestressed Concrete Institute, Chicago, Illinois, 1978, pp. 1-1 to 8-28.
8. *Standard Specifications for Highway Bridges*, American Association of State Highway and Transportation Officials (AASHTO), Washington, D.C., 1977, pp. 1-496.
9. *Code for the Design of Concrete Structures for Buildings*, CAN3-A23.3-M77, Canadian Standards Association (CSA), Ottawa, Canada, 1977.
10. Branson, D. E., and Trost, H., "Unified Procedures for Predicting the Deflection and Centroidal Axis Location of Nonprestressed and Partially Prestressed Members," *Lehrstuhl und Institut für Massivbau*, Technische Hochschule (RWTH) Aachen, June 1981, pp. 1-118.
11. Branson, D. E., and Trost, H., "Unified Procedures for Predicting the Deflection and Centroidal Axis Location of Partially Cracked Nonprestressed and Prestressed Concrete Members," *ACI Journal*, Proceedings, V. 79, No. 2, March-April 1982, pp. 119-130.
12. Bennett, E. W., Discussion of "Design of Partially Prestressed Concrete Flexural Members," by S. E. Moustafa, PCI JOURNAL, V. 22, No. 3, May-June 1977, pp. 12-29. Discussion in PCI JOURNAL, V. 23, No. 3, May-June 1978, pp. 92-94.
13. Tadros, M. K., "Designing for Deflection," Advanced Design Seminar, 1979 PCI Convention, (unpublished manuscript), pp. 1-25.
14. Newmark, N. M., "Numerical Procedure for Computing Deflections, Moments, and Buckling Loads," *Transactions, ASCE*, 1-8, 1943, pp. 1161-1234.